



Molecular Imaging and the PD-L1 Pathway: From Bench to Clinic

David Leung¹, Samuel Bonacorsi¹, Ralph Adam Smith¹, Wolfgang Weber^{2*} and Wendy Hayes¹

¹ Translational Medicine, Bristol Myers Squibb, Princeton, NJ, United States, ² Technische Klinikum rechts der Isar, Technical University of Munich, Munich, Germany

OPEN ACCESS

Edited by:

Freimut Dankwart Juengling,
University of Alberta, Canada

Reviewed by:

Niklaus Schaefer,
Centre Hospitalier Universitaire
Vaudois (CHUV), Switzerland
Laurence Gluch,
The Strathfield Breast Centre,
Australia

*Correspondence:

Wolfgang Weber
w.weber@tum.de

Specialty section:

This article was submitted to
Cancer Imaging and
Image-directed Interventions,
a section of the journal
Frontiers in Oncology

Received: 21 April 2021

Accepted: 22 July 2021

Published: 23 August 2021

Citation:

Leung D, Bonacorsi S, Smith RA,
Weber W and Hayes W (2021)
Molecular Imaging and the PD-L1
Pathway: From Bench to Clinic.
Front. Oncol. 11:698425.
doi: 10.3389/fonc.2021.698425

Programmed death-1 (PD-1) and programmed death ligand 1 (PD-L1) inhibitors target the important molecular interplay between PD-1 and PD-L1, a key pathway contributing to immune evasion in the tumor microenvironment (TME). Long-term clinical benefit has been observed in patients receiving PD-(L)1 inhibitors, alone and in combination with other treatments, across multiple tumor types. PD-L1 expression has been associated with response to immune checkpoint inhibitors, and treatment strategies are often guided by immunohistochemistry-based diagnostic tests assessing expression of PD-L1. However, challenges related to the implementation, interpretation, and clinical utility of PD-L1 diagnostic tests have led to an increasing number of preclinical and clinical studies exploring interrogation of the TME by real-time imaging of PD-(L)1 expression by positron emission tomography (PET). PET imaging utilizes radiolabeled molecules to non-invasively assess PD-(L)1 expression spatially and temporally. Several PD-(L)1 PET tracers have been tested in preclinical and clinical studies, with clinical trials in progress to assess their use in a number of cancer types. This review will showcase the development of PD-(L)1 PET tracers from preclinical studies through to clinical use, and will explore the opportunities in drug development and possible future clinical implementation.

Keywords: molecular imaging, PD-L1, PET tracer, radioisotope, ¹⁸F-fluorodeoxyglucose

INTRODUCTION

Programmed death-1 (PD-1) and programmed death ligand 1 (PD-L1) checkpoint inhibition plays a critical part in improving prognoses for patients with a range of tumor types (1). The immunosuppressive PD-1 receptor, expressed on various immune cells, including activated T cells, regulatory T cells, monocytes, and dendritic cells, is the target of a number of immune checkpoint inhibitors (ICIs), such as nivolumab and pembrolizumab (2). These treatments, together with those targeting the ligand PD-L1, which is expressed on both immune cells and tumor cells (3), increasingly form the backbone of immunotherapy for a variety of tumor types and disease stages (4). Optimization of these therapies relies on targeting patients who will most likely benefit from treatment (5). To achieve this goal, a better understanding of the underlying tumor biology is needed. Interrogation of the tumor microenvironment (TME) reveals considerable interplay between PD-1 and PD-L1 signaling (6), and although multiple molecules contribute to this immunosuppressive milieu, PD-L1 expression in some tumors is the single biomarker most closely associated with response to PD-1 blockade (6–8). Recent data indicate that low

expression of PD-1 may also be associated with response to PD-1 blockade (9), although this requires further investigation.

PD-L1 expression may be predictive of benefit with ICIs (5). Currently, PD-L1 expression is assessed by immunohistochemistry (IHC) from tissue samples and is reported as a numerical value (percent positive tumor or immune cells). Therefore, a given result can only represent PD-L1 expression of a small portion of a selected tumor, and there are frequently multiple tumors (e.g., primary and metastatic sites) in the same patient that are not assessed (10). A way to start addressing this shortcoming is molecular imaging. Molecular imaging most commonly utilizes positron or single-photon emitting radionuclides to label specific targets, such as PD-(L)1 binding molecules, for *in vivo* visualization purposes (11–19). Using these positron emission tomography (PET) and single-photon emission computed tomography (SPECT) imaging techniques, PD-(L)1 expression of not just one part of a tumor, but of the entire tumor burden, can be assessed non-invasively (20, 21). Furthermore, molecular imaging allows serial monitoring of PD-(L)1 expression over time (20, 21), whereas temporal assessment by IHC is much more challenging clinically due to the requirement for multiple invasive biopsies (20, 21). In addition to safety considerations, other known limitations of IHC that could impact treatment decisions may include interobserver and intraobserver reproducibility, variability due to fresh vs. archival biopsied tissue (10, 22–24), and heterogeneity of expression within and among tumors (25, 26).

Molecular imaging therefore holds promise for *in vivo* quantification of PD-(L)1 expression in tumors and healthy tissue, as well as assessment of drug pharmacokinetics and pharmacodynamics (27), which will provide insights into the mechanisms of ICIs and ultimately improve patient selection, monitoring, and treatment (20, 21, 28). This review discusses the evolution of PD-(L)1 imaging from preclinical studies to current and potential future use in drug development and clinical settings, highlighting the opportunities for PD-(L)1 molecular imaging to improve healthcare outcomes.

THE RATIONALE FOR MOLECULAR IMAGING OF PD-(L)1: ENHANCING AND COMPLEMENTING CURRENT IHC ASSESSMENT OF PD-L1 EXPRESSION

Regulatory approvals of PD-(L)1 inhibitors have been accompanied by several companion or complementary IHC diagnostic tests to assess PD-L1 expression (5, 10, 29). However, methodological variations in scoring algorithms, cell types assessed (tumor cells, immune cells, or both) and expression cutoffs, as well as interobserver variabilities, can hinder data interpretation and reliability (30–32). Furthermore, heterogeneity in tumor PD-L1 expression within a tumor and among tumors within the same patient adds biological variation (26, 33). For example, Munari et al. showed that four or more biopsies were required to accurately evaluate and classify PD-L1 expression using IHC in patients with non-small cell lung cancer (NSCLC) (26). The situation is further complicated by the choice

of tissue sample, with poor concordance between results derived from biopsy sections and whole tissue samples (25). Given the limitations associated with IHC-based PD-L1 assessment, alternative techniques such as molecular imaging and artificial intelligence (AI)-based digital pathology are being developed (20, 21, 28, 34).

Clinical Utility of Current PET Tracers

PET imaging with the glucose analogue ^{18}F -fluorodeoxyglucose (^{18}F -FDG) is a technically mature imaging technique, and is a standard of care that is routinely employed for the diagnosis and monitoring of patients with cancer (35–38). In the context of immunotherapy, high pretreatment ^{18}F -FDG uptake was associated with decreased duration of response and overall survival to ICIs in patients with melanoma (39, 40). In addition, on-treatment decreases in ^{18}F -FDG uptake have been used as an early surrogate for clinical benefit (41, 42). For example, lower total lesion glycolysis and metabolic tumor volume (MTV), as determined in patients with NSCLC using ^{18}F -FDG PET, have been shown to be prognostic and predictive of response and longer overall survival following nivolumab or pembrolizumab monotherapy (43–46). A metabolic score derived from combined assessment of pretreatment MTV and the neutrophil-to-lymphocyte ratio may provide a more accurate prediction of outcome than either of these factors alone (47, 48). Furthermore, in patients with NSCLC, the maximal standard uptake value (SUV) of ^{18}F -FDG has been reported to be positively associated with PD-L1 expression (49, 50), and high ^{18}F -FDG MTV is associated with PD-L1 expression $\geq 75\%$ (48). However, ^{18}F -FDG PET imaging, like computed tomography (CT), can show pseudoprogression (an early increase in tumor volume and FDG uptake on imaging with a subsequent favorable response to ICI therapy) (51, 52). Pseudoprogression is not common (approximately 5% of patients, according to current estimates) (53) but can potentially result in stopping effective therapy in individual patients (52). ^{18}F -FDG PET has also shown promise in predicting response and overall survival in malignant melanoma and relapsed or refractory Hodgkin lymphoma after treatment with nivolumab and ipilimumab, an anti-cytotoxic T lymphocyte antigen-4 therapy (40, 54–56). Together, these studies indicate that ^{18}F -FDG may facilitate the identification of patients most likely to benefit from ICIs (57). A number of novel PET tracers, such as ^{11}C -choline, have also been investigated clinically and are reviewed in detail elsewhere (35, 36, 58, 59).

Within oncology, PET tracers allow the monitoring of biomarkers, such as PD-(L)1, across the whole body and over a treatment course, without the need for multiple biopsies (21, 60). The ability for isotopes to be conjugated to therapeutic antibodies, such as ^{89}Zr -trastuzumab or ^{89}Zr -nivolumab, may help to assess their pharmacokinetics. Studies have shown that patients who were trastuzumab-naïve cleared ^{89}Zr -trastuzumab at a faster rate than patients previously treated with trastuzumab (61, 62). A similar finding might be expected in patients being retreated or rechallenged with ICIs (63), an emerging patient population in the immunotherapy arena. A better understanding of the uptake and distribution of drugs/molecules and their

mechanisms of action using molecular imaging may lead to earlier identification of potentially effective therapies and a consequent reduction in drug development costs (64, 65).

Clinical Interrogation of PD-(L)1 PET Tracers

To understand the rationale of how specific PD-(L)1 molecular imaging may enhance and complement current IHC assessment of PD-L1 expression, it is important to consider in more depth the different advantages, limitations, and technical challenges of both techniques (**Figure 1**) (2, 20, 21, 30–32, 65–70).

It is likely that the most effective use of these techniques will be through a combination of the complementary information provided (71). Both IHC (30–32) and PET (71–73) are associated with issues regarding standardization of analysis and interpretation of results. PET imaging is less prone to preanalytical factors such as fresh vs. archival tissue samples, which may affect PD-L1 IHC assessment (74), or analytical factors such as different staining patterns between IHC assays (31). On the other hand, one tissue sample collected for IHC analysis can support evaluation of multiple biomarkers, cell morphology, and elements of the tumor and TME (21). Together, these technologies can augment each other: cellular and subcellular details from IHC complement the

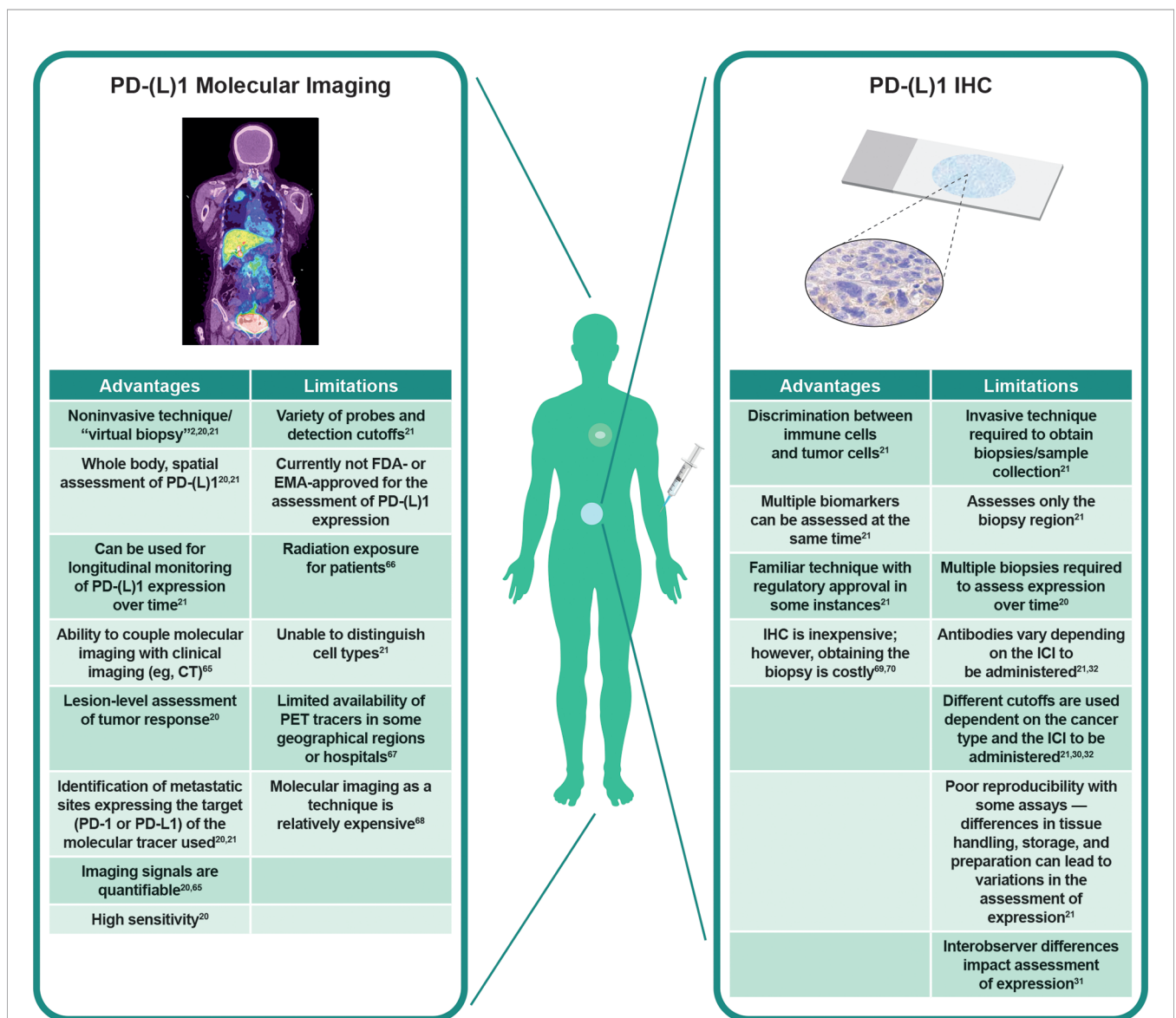


FIGURE 1 | Visualization of PD-L1 expression at tumor sites. Left panel: PD-L1 PET tracers can be used to visualize and monitor PD-L1 expression at all tumor sites. Right panel: IHC can be used to assess PD-L1 expression at the biopsy site, representing a small region of only one tumor. Adapted from Du et al. (2) and Broos et al. (21). CT, computed tomography; EMA, European Medicines Agency; FDA, Food and Drug Administration; ICI, immune checkpoint inhibitor; IHC, immunohistochemistry; PD-1, programmed death-1; PD-L1, programmed death ligand 1; PET, positron emission tomography.

whole-body evaluation of tumor PD-(L)1 expression from molecular imaging (21). Imaging can thus serve as a “virtual biopsy” when tissue sampling is challenging; for example, during treatment or when the location of the tumor is unsafe for sampling.

Because cell types cannot be determined using PET, PD-L1 IHC and PD-L1 PET will likely become better aligned in IHC assays that assess PD-L1 expression on tumor and immune cells using the combined positive score algorithm (75, 76). With this in mind, we are optimistic that use of these techniques side by side will guide clinical decision-making in the future (76).

CONSIDERATIONS FOR THE DEVELOPMENT AND USE OF PD-(L)1 PET TRACERS

Considerations in developing molecular imaging agents such as PD-(L)1 PET tracers include the requirement for high target specificity and affinity as well as adequate tumor penetration of the tracer (77, 78). Furthermore, tracer uptake should have sufficient resolution to assess potential heterogeneity within each lesion and among lesions from the same patient (71–73).

Maute et al. (77) addressed affinity, specificity, and tumor penetration when determining whether PD-(L)1-directed immunotherapy could be improved with smaller, non-antibody therapeutics that could be radiolabeled and applied as a PET tracer. Binding affinity was investigated by identifying the key amino acid residues in the PD-1 ectodomain that are important to PD-1:PD-L1 interaction. The authors then engineered a high-affinity PD-1 variant (high-affinity consensus [HAC] PD-1) *via* selection of optimized mutation combinations, which led to a 15,000–40,000-fold increase in affinity and an increase in the half-life of the PD-1:PD-L1 interaction from ≤ 1 second to ~ 40 minutes (77).

A high degree of specificity of the radiolabeled ^{64}Cu -DOTA-HAC-PD-1 for PD-L1 binding was confirmed by the lack of signal within PD-L1-negative tumors or in human PD-L1-positive tumors blocked by prior injection of unlabeled HAC-PD-1.

Due to its smaller size, tumor penetration was enhanced with ^{64}Cu -DOTA-HAC-PD-1, showing binding to PD-L1 on tumor cells that appeared to be inaccessible to larger antibody binding (77). However, target binding affinity and specificity are only two factors influencing biodistribution of protein-based PET tracers *in vivo*. Other factors include protein size and glycosylation, metabolic stability, chelators, and the radiometal used for labeling (78, 79). The contribution of these factors on uptake by target and non-target tissues is complex and must be determined experimentally (78).

The choice of radionuclide deserves specific discussion. The half-life of the radionuclide on the molecular imaging agent needs to be compatible with the time needed for binding of the molecular target, while maintaining suitable levels of radioactivity to allow reasonable imaging resolution (80). Small biologics such as antibody fragments and adnectins show rapid

distribution from vasculature to tissues (81, 82). An isotope with a short half-life (minutes to hours) is optimal (80), and imaging can typically occur during or soon after tracer administration. For example, ^{11}C -acetate, originally employed in cardiology but now being used in oncology (in particular prostate cancer), has a physical half-life of approximately 20 minutes, and imaging is acquired shortly after tracer infusion (83, 84).

Clinical ^{18}F -FDG PET (85) and ^{18}F -BMS-986192 (72, 86) imaging of PD-L1 are both assessed at 60 minutes post-injection. Conversely, imaging with antibodies (e.g., ^{89}Zr -labeled nivolumab) is best achieved 5 to 7 days post-tracer injection (72). However, imaging several days after tracer injection is inconvenient for the patient and makes it difficult to assess more rapid changes in the density of the target, as the tumor uptake on PET reflects the average density of the target during a period of 5 to 7 days. Furthermore, long-lived radioisotopes, such as ^{89}Zr , cause a several-fold higher radiation exposure to normal organs than ^{18}F (87). However, new total-body PET scanners will make it feasible to acquire PET scans with ^{89}Zr -labeled radiotracers ~ 30 days after injection, and could allow for the radioactivity administered to be reduced by a factor of 40 (88–90).

In some instances, accumulation of tracers may be anticipated in a well-perfused physiological “antigen sink”, such as the spleen, which may result in insufficient uptake of the tracer in the tumor tissue (91). Co-administration of unlabeled versions of tracer may need to be investigated to reduce accumulation of the labeled tracer in antigen sinks (11). If the imaging agent is derived from a therapeutic agent (11), an analogous investigation may be warranted.

The dynamic range of a tracer is a further parameter to consider, as is the proportion of signal alteration that can occur under a perturbed system; for example, altered expression of a biomarker in a disease state. A high dynamic range allows smaller alterations to be accurately detected, thus increasing sensitivity (92). In general, PET is considered to be better suited than SPECT for tracer quantification and in dynamic imaging (65). SPECT is markedly less sensitive than PET and accurate quantification of activity concentrations is challenging (65). Due to lower sensitivity, SPECT scans take longer than PET scans (93); therefore, as a result of the additional burden on patients and resources, repeated SPECT imaging may be less well tolerated than repeated PET scans. The dynamic process of tracer uptake and retention can be better assessed through a time series of images during dynamic imaging, as opposed to a single time point from a static image (94).

In addition to the biological and chemical considerations around development of a PET tracer, it is important to describe the quantification procedure, including reporting SUVs or tumor:blood pool ratios, for example (71–73). However, the uptake of a radiotracer depends not only on binding to its target (specific uptake), but also on other mechanisms (non-specific uptake) (95). Therefore, quantifying target expression with a simple image-derived parameter such as an SUV or a tumor:blood pool ratio may not be optimal. Dynamic whole-

body imaging, in contrast to static imaging, can often produce multiparametric images of influx rate and distribution volume while also providing conventional “SUV” equivalents (96). Systematic studies are needed to provide a quantitative parameter to allow for a best estimation of tracer concentration in the target tissue.

FROM PRECLINICAL TO CLINICAL STUDIES USING PD-(L)1 PET TRACERS

The *in vitro* and *in vivo* preclinical models used to test PD-(L)1 PET tracers have grown in complexity, from early studies using cell-line-based systems and mouse models (14, 16, 19, 77), including xenografts and other tumor models, to more recent studies using healthy non-human primates (11, 12) (**Supplementary Table 1**). Results from preclinical studies of PD-(L)1 PET tracers have been encouraging, with tracers demonstrating specific binding and the ability to detect varying levels of PD-(L)1 expression, including endogenous expression (14, 17–19, 77, 97, 98). Studies in more complex systems such as non-human primates have involved both ^{18}F -BMS-986192, an ^{18}F -fluorine labeled anti-PD-L1 adnectin small molecule, and ^{89}Zr -nivolumab (11, 12). Further imaging studies in healthy cynomolgus monkeys using ^{18}F -BMS-986192 and ^{89}Zr -nivolumab, which specifically bind to PD-L1 and PD-1, respectively, have begun to directly investigate whether PD-(L)1 imaging could be a viable option for imaging in humans (11, 12). As noted, binding of ^{89}Zr -nivolumab in the PD-1-rich spleen “antigen sink” could be reduced by co-administration of unlabeled nivolumab (11). ^{18}F -BMS-986192 has low to moderate uptake in the lungs, heart, liver, and muscles. This biodistribution allows good contrast with PD-L1-positive tumors (12). ^{18}F -BMS-986192 does have an expected higher tracer uptake in the spleen and in urinary structures (excretion pathway), although these are not common organs of metastatic disease in solid tumors. Radiation dosimetry indicated that this tracer was safe to administer in humans (12).

These preclinical studies suggest that PD-(L)1 PET imaging is a viable technique to assess PD-(L)1 expression in humans, and PD-(L)1 PET tracers have progressed into first-in-human studies (**Table 1**). These first-in-human studies have provided insights into various aspects of molecular imaging, including biodistribution, intratumoral and intertumoral heterogeneity, and preliminary safety findings, including those indicating a lack of toxicity (71–73, 100).

In terms of biodistribution, accumulation in the spleen and bone marrow is an expected feature of PD-(L)1-targeting agents (11, 16, 101). As mentioned, the accumulation of antibodies in “antigen sinks”, such as the spleen, may require the use of an unlabeled version to block antibody binding sites to allow more of the labeled tracer to reach the tumor (11, 16, 101). First-in-human PET with ^{18}F -BMS-986192 and ^{89}Zr -nivolumab reported tracer uptake in the spleen and marrow (72). Whole-body PD-(L)1 PET-CT with ^{89}Zr -atezolizumab also accumulated in the spleen, with uptake also occurring in the bone marrow over time (73).

In contrast, the accumulation of tracers is low in the lung and absent in healthy brain (11, 12, 72).

Although PD-(L)1 PET tracers have not been shown to accumulate in the brain (72, 73), a key outstanding question is whether PD-(L)1 PET can be used to image brain metastases that typically cause a disruption in the blood–brain barrier. Central nervous system uptake of ^{18}F -BMS-986192 and ^{89}Zr -nivolumab was observed in some, but not all, of the untreated brain metastases in two patients enrolled in the first-in-human study (72). Further studies addressing the ability of tracers to cross the blood–brain barrier will be required and should ideally include pathologic correlations.

Given the spatial and temporal nature of molecular imaging, an additional benefit for patient outcomes is the identification of multiple tumor sites. Results from first-in-human trials using ^{89}Zr -atezolizumab, ^{18}F -BMS-986192, ^{89}Zr -nivolumab, and $^{99\text{m}}\text{Tc}$ -NM-01 indicated that PET tracers can also be used for the visualization of multiple lesions expressing PD-(L)1 (71–73). Tracer uptake heterogeneity was found to be relatively common among metastases (71, 72).

Alongside biodistribution data in humans, safety data are also imperative. Toxicity and safety data from the first-in-human studies revealed no reported tracer-related adverse events for ^{18}F -BMS-986192, ^{89}Zr -nivolumab (72), or $^{99\text{m}}\text{Tc}$ -NM-01 (71), although one grade 3 infusion-related adverse reaction was reported in the first-in-human study using ^{89}Zr -atezolizumab (73).

Given the association between IHC-determined PD-L1 expression and response to ICIs, it is crucial to demonstrate that a similar relationship exists for molecular imaging. Although there are limited data available showing association of PD-L1 expression assessed by molecular imaging with efficacy, encouraging results were provided by the first-in-human study of ^{89}Zr -atezolizumab, in which clinical response was better correlated with pretreatment PET-imaging-assessed PD-L1 expression compared with either IHC-based or RNA-sequencing-based PD-L1 assays (73). Similarly, Niemeijer et al. demonstrated that PD-(L)1 PET imaging can predict lesion-level response (**Table 1**) (72). Moreover, tumors determined to be PD-L1-positive by IHC and PET accumulate nivolumab, while PD-L1-negative tumors do not (72). These findings demonstrate that tumors that use PD-L1 for immune escape can be readily targeted by nivolumab immune blockade (72). This also suggests that PD-L1 determination by molecular imaging or other methods may facilitate the selection of patients who are most likely to respond to treatment with ICIs.

Affirming the Use of PD-L1 PET Tracers in Clinical Studies: Assessment of PD-L1 Expression by IHC and Molecular Imaging

It is of interest to assess whether any new PD-L1 assessment using molecular imaging in preclinical and clinical studies shows consistent imaging and biodistribution of PD-L1 when compared with the current standard assessment by IHC, taking into consideration the nuances and variations already described with IHC analyses. Agreement between PD-L1 IHC and molecular imaging has been assessed in a number of

TABLE 1 | Examples of clinically tested PD-(L)1 PET tracers.

Author, year	Tracer	Biodistribution/accumulation	Key findings
Niemeijer et al., 2018 (72)	¹⁸ F-BMS-986192 ⁸⁹ Zr-nivolumab	Both tracers showed high accumulation in the spleen and liver. ¹⁸ F-BMS-986192 showed some uptake in the hypophysis	<ul style="list-style-type: none"> No tracer-related adverse events of grade ≥ 3 No accumulation of ¹⁸F-BMS-986192 and ⁸⁹Zr-nivolumab occurred in normal brain Heterogeneity in the uptake of ¹⁸F-BMS-986192 occurred between and within patients Accumulation of ¹⁸F-BMS-986192 and ⁸⁹Zr-nivolumab was seen in some, but not all, brain metastases ¹⁸F-BMS-986192 uptake in tumor lesions correlated with PD-L1 expression assessed using IHC. The uptake of ⁸⁹Zr-nivolumab correlated with PD-1-positive, tumor-infiltrating immune cells Response to nivolumab evaluation on a lesional basis (excluding lesions <20 mm diameter) showed that ¹⁸F-BMS-986192 SUV_{peak} was higher for responding lesions than non-responding lesions (median 6.5 vs. 3.2, $P = 0.03$, Mann-Whitney U-test) (analogous lesional correlation for ⁸⁹Zr-nivolumab median SUV_{peak} 6.4 vs. 3.9, $P = 0.019$, Mann-Whitney U-test)
Bensch et al., 2018 (73)	⁸⁹ Zr-atezolizumab	High uptake over time occurred in the intestines, kidneys, and liver. Low uptake occurred in the brain, subcutaneous tissue, muscle, compact bone, and lungs	<ul style="list-style-type: none"> Lesions at all main metastatic sites were visualized The detection of CNS lesions was not determined, as patients with CNS metastases were excluded from the study Within-patient heterogeneity was observed in patients with >1 lesion Heterogeneous intratumor tracer uptake was observed One low-grade adverse event was reported ⁸⁹Zr-atezolizumab uptake increased with SP142-assessed PD-L1 staining, but not with SP263-assessed PD-L1 expression
Xing et al., 2019 (71)	^{99m} Tc-NM-01	Biodistribution was observed in the kidneys, liver, and spleen, and to a lesser extent in the bone marrow and lungs, reflecting the physiological expression of PD-L1	<ul style="list-style-type: none"> Intratumoral and intertumoral heterogeneity was observed Acceptable dosimetry was reported, with levels similar to other agents in clinical use No drug-related adverse events were reported Primary tumor:blood pool ratios at 2 h correlated with IHC
Verhoeff et al., 2020 (99)	⁸⁹ Zr-durvalumab	High ⁸⁹ Zr-durvalumab retention was observed in the spleen and liver	<ul style="list-style-type: none"> Heterogeneous accumulation was observed within tumors and between patients Uptake of ⁸⁹Zr-durvalumab was not seen in all ¹⁸F-FDG-positive tumors No correlation between tumor PD-L1 expression determined using ⁸⁹Zr-durvalumab uptake and PD-L1 expression on archival tissue was found In PD-L1-positive lesions, time-activity curves for ¹⁸F-BMS-986192 increased over time, while for PD-L1-negative tumors the time-activity curves remained approximately flat up to 40 minutes post-injection At 60 min post-injection, in 61% of the tumors analyzed, the uptake of ¹⁸F-BMS-986192 was best described by a reversible single-tissue model. In 39% of the tumors analyzed, including in one lesion with a 10% positive IHC score and in one lesion with a negative IHC score, an irreversible two-tissue model was preferred SUV normalized to injected activity over body weight correlated best with the distribution volume of ¹⁸F-BMS-986192
Huisman et al., 2020 (100)	¹⁸ F-BMS-986192	–	<ul style="list-style-type: none"> In PD-L1-positive lesions, time-activity curves for ¹⁸F-BMS-986192 increased over time, while for PD-L1-negative tumors the time-activity curves remained approximately flat up to 40 minutes post-injection At 60 min post-injection, in 61% of the tumors analyzed, the uptake of ¹⁸F-BMS-986192 was best described by a reversible single-tissue model. In 39% of the tumors analyzed, including in one lesion with a 10% positive IHC score and in one lesion with a negative IHC score, an irreversible two-tissue model was preferred SUV normalized to injected activity over body weight correlated best with the distribution volume of ¹⁸F-BMS-986192

CNS, central nervous system; FDG, fluorodeoxyglucose; IHC, immunohistochemistry; PD-1, programmed death-1; PD-L1, programmed death ligand 1; PET, positron emission tomography; SUV, standard uptake value.

preclinical studies and has generally been found to be high, although most studies do not report statistical concordance assessments (12, 13, 17–19). This includes results with the PD-L1 PET tracers ¹¹¹In-MPDL3280A and NIR-MPDL3280A in triple-negative breast cancer (TNBC) and NSCLC xenografts (19), and with ¹⁸F-BMS-986192 in NSCLC (12). Consistent imaging and biodistribution was also reported between IHC-determined PD-L1 expression and the uptake of the PD-L1 PET tracer ¹¹¹In-DTPA-anti-PD-L1 in xenografts and mouse models (16).

Correlation between PD-L1 imaging and IHC was reported in the first-in-human trials (71–73). Niemeijer et al, in a study assessing the entire PD-1 and PD-L1 pathway, reported correlation of the PET signal of ¹⁸F-BMS-986192 with PD-L1 IHC and of the ⁸⁹Zr-nivolumab PET signal with PD-1 IHC. The median ¹⁸F-BMS-986192 SUV_{peak} was higher for lesions with $\geq 50\%$ tumor PD-L1 expression by IHC than for lesions with <50% (8.2 vs. 2.9, $P = 0.018$, Mann-Whitney U-test) (72).

In a study by Bensch et al. (73), uptake of ⁸⁹Zr-atezolizumab was higher in lesions with IHC-determined PD-L1 expression than in those without. However, this was only the case with the Ventana PD-L1 (SP142) assay, not the Ventana PD-L1 (SP263) assay, highlighting that variations among IHC assays should be taken into consideration. This study also found that tracer uptake differed between tumor types, with TNBC showing an average 50% less uptake than locally advanced or metastatic bladder cancer (73). Tumor vascularity may be related to tracer uptake and could account for some uptake differences between tumor types (102). Concordance between primary tumor:blood pool ratios of a SPECT-based tracer and IHC has also been reported, with primary tumor:blood pool ratios at 2 hours correlating with PD-L1 IHC ($r = 0.68$, $P = 0.014$) (71). Dosimetry for ^{99m}Tc-NM-01 was reported to be similar to other SPECT agents in clinical use (71), indicating that the use of ^{99m}Tc-NM-01 in patients is feasible. Furthermore, quantitative assessment with this tracer in patients with NSCLC has been demonstrated to be reproducible

and reliable between independent observers (103). The results from these studies indicate that PD-(L)1 molecular imaging generally shows concordance with IHC-based PD-L1 expression. However, as concordance was not observed in all studies, some caution is required.

The Growing Momentum for PD-(L)1 Molecular Imaging Clinical Studies

Several clinical trials evaluating the potential roles of PD-(L)1 PET tracers in assessing PD-(L)1 expression are recruiting or active. Although trials were initially undertaken in NSCLC, the progression of ICI use into other tumor types has seen the expansion of PD-(L)1 PET tracer studies into squamous cell carcinoma of the head and neck, breast cancer, renal cell carcinoma, diffuse large B-cell lymphoma, melanoma, and other cancers (**Figure 2** and **Supplementary Table 2**). These trials aim to validate the initial proof-of-principle, first-in-human studies with larger datasets. The majority are being performed in single or multiple institutions with industry sponsorship; however, for rare tumors, collaborative groups across multiple institutions may be advantageous. Depending on the critical clinical question being addressed, the trial design may vary. Studies addressing pharmacodynamic changes of a biomarker will need to have multiple scanning time points (e.g., NCT03850028; **Supplementary Table 2**), whereas those that aim for baseline biodistribution may have a single scan (e.g., NCT03564197, NCT02978196; **Supplementary Table 2**).

The further development of PD-(L)1 molecular imaging as a clinical research tool and biomarker requires several important steps. The first is a body of evidence supporting the clinical utility

of PD-L1 PET as a diagnostic tool and comparing it with standard methods for evaluating PD-L1, such as IHC. Several prospective trials are ongoing to determine a predictive or prognostic benefit of molecular imaging for ICI therapy (e.g., NCT03514719, NCT03564197, and NCT03843515; **Supplementary Table 2**). Second, there is a need to adopt standardized imaging protocols and criteria for quantitative image analysis (57). Involvement of industry collaborations or large institutions may be necessary to acquire the necessary data and achieve harmonization. Third, as noted above, imaging with radiolabeled antibodies results in effective radiation doses that are several-fold higher than for PET imaging agents, such as ^{18}F -FDG and ^{68}Ga -DOTA-TATE (104). These radiation doses may limit broader use of PD-(L)1 imaging, especially for serial PET scans to monitor changes in PD-(L)1 expression in individual patients. Development of PET imaging agents labeled with short-lived positron emitters, such as ^{18}F or ^{68}Ga , is a highly active research field with encouraging preclinical and clinical results (12, 72, 105). PET imaging studies generally use micro-dosing, defined as less than one hundredth of the dose that has a pharmacological effect, to a maximum of 100 μg , which is considered to have a very limited risk to participants (106). This strategy is used in NCT02978196, for example (**Supplementary Table 2**). Further trials should follow guidelines, such as those provided by the United States Food and Drug Administration for radiolabeled PET tracers (106), to be approved for clinical implementation. It is anticipated that ongoing and future trials will provide the solid body of evidence necessary to develop guidelines for the adoption of molecular imaging into routine clinical practice.

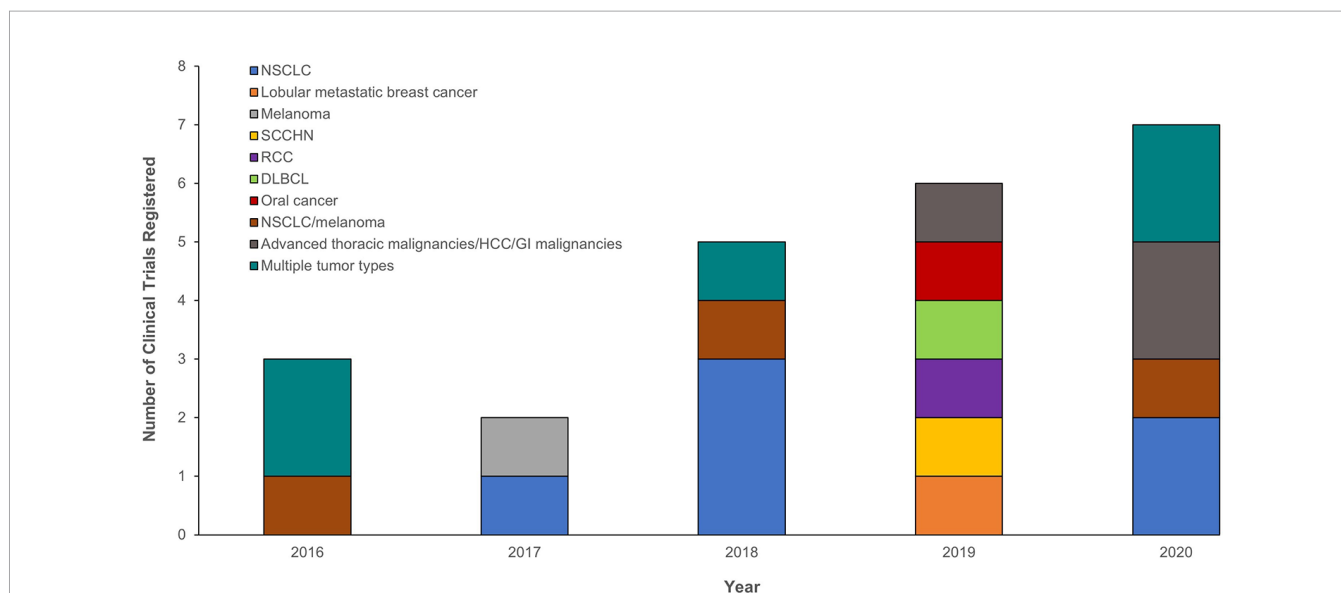


FIGURE 2 | Registered clinical trials between 2016 and 2020 evaluating the potential role of PD-(L)1 PET tracers in assessing PD-(L)1 expression and the tumor types investigated. Only trials registered with ClinicalTrials.gov are presented at the year the trial was initiated. The following search term was used for each year: ("nuclear medicine" OR imaging OR 89Zr OR 18F OR 99mTc) AND (PD-L1 OR PD-1 OR anti-PD-L1 OR anti-PD-1). DLBCL, diffuse large B-cell lymphoma; GI, gastrointestinal; HCC, hepatocellular carcinoma; NSCLC, non-small cell lung cancer; PD-1, programmed death-1; PD-L1, programmed death ligand 1; PET, positron emission tomography; RCC, renal cell carcinoma; SCCHN, squamous cell carcinoma of the head and neck.

DISCUSSION

There are opportunities and challenges facing the incorporation of molecular imaging for PD-(L)1 expression into drug development and routine clinical practice. Some of the key scientific questions relating to safety, correlation with IHC, and prediction of patient outcome are being investigated, as summarized above. Data from studies investigating the impact of PD-(L)1 imaging on patient outcomes are not yet available. For broader clinical use of PD-(L)1 imaging, it will be necessary to show that patient selection by PD-(L)1 molecular imaging results in equivalent or better patient outcomes than selection by IHC. Since molecular imaging offers non-invasive, real-time measurement of biomarkers, it may overcome the issues of dynamic changes in PD-L1 expression, which are often highlighted as the major challenge associated with this biomarker (1, 57, 97). Once this is established by prospective clinical trials, dissemination of PD-(L)1 imaging could likely be achieved relatively quickly because PET/CT imaging is technically mature and already in routine clinical use (67), minimizing the need for expensive equipment investment and extensive personnel training. Furthermore, in many countries there is already a well-established infrastructure for production and regional distribution of PET radiopharmaceuticals, such as ^{18}F -FDG and ^{68}Ga -DOTA-TATE (107, 108). This infrastructure could very likely also provide PD-(L)1 imaging agents to centers that provide PD-(L)1-targeted therapies. Global harmonization and approvals of imaging tests across regulatory bodies (109), as well as validation and standardization of PD-(L)1 imaging techniques, will be important for the technique to gain widespread usage. Once implemented into clinical practice, molecular imaging is anticipated to improve patient care by minimizing ineffective therapy and over- or under-treatment. Early termination of clinical trials with drug candidates that have been identified as having poor safety or efficacy by molecular imaging is another area where these techniques can provide value.

Taking these challenges into consideration, there is a wealth of opportunity to expand the use of molecular imaging. Further advances are likely to take advantage of sequential PET tracer combinations; for example, to assess the expression of PD-L1 and of PD-1, as was carried out in the study conducted by Niemeijer et al. (72). Sequential PET tracer combinations have also been used to assess the correlation between metabolic activity and histopathology in glioma (110), and to assess myocardial viability and perfusion (111). Using combinations of tracers in such a way may allow a more comprehensive interrogation of selected (patho)physiology.

There may also be a role for PD-(L)1 PET tracers in characterizing changes in the TME in order to assess tumor progression, inflammatory responses, or drug resistance. For example, the radiation-associated abscopal effect can lead to T-cell infiltration of the TME by increasing the release of chemokines and expression of adhesion molecules, and upregulating class I major histocompatibility complexes, leading to immunologically cold tumors becoming

immunologically hot tumors (112, 113). In this way, seemingly ICI-resistant tumors may begin to respond to such treatments. PD-(L)1 imaging could be used to visualize such events, allowing for a better understanding of the mechanisms of immunoncology and the principles underlying ICI/radiation combination therapies (113). Furthermore, by allowing the possibility to assess PD-(L)1 expression longitudinally and enabling the TME to be interrogated, molecular imaging is expected to facilitate the visualization of immunosuppressive cells, which may allow different types of progression, such as true progression and pseudoprogression, to be distinguished (57). However, given the complexity of the human immune system, a full understanding of the dynamic tumor microenvironment and the antitumor immune response will require comprehensive evaluation of other immune components in addition to PD-(L)1. Evaluation of cytokine signaling with a radiolabeled transforming growth factor (TGF)- β inhibitor, and SPECT imaging of tumor-infiltrating lymphocytes (with $^{99\text{m}}\text{Tc}$ -labeled interleukin-2), regulatory T cells, and tumor-associated macrophages, are some of the developments beyond PD-(L)1 imaging that could contribute to improved assessment of response to ICI therapy and subsequent clinical management (42, 57).

It is likely that the role of molecular imaging for assessment of PD-(L)1 expression in a clinical setting will evolve alongside improved understanding of the PD-(L)1 pathway and other related immunobiology and biomarker technologies. Investigations have already pointed to the possible role of soluble PD-(L)1 detection in patient serum/plasma (114) and the use of AI-based digital pathology to assess PD-L1 expression (115, 116). The potential to multiplex these technologies will facilitate the acquisition of complex anatomic and pathologic patient data (34, 76). Molecular imaging may also be used in conjunction with other diagnostic methods, such as genomic and transcriptomic profiling, increasing the breadth of biological knowledge a clinician can obtain from a patient and aiding treatment strategies.

Molecular imaging, including PD-(L)1 PET imaging, will likely gain a more influential role in drug development in the future. Molecular imaging may be used in early-phase clinical trials to facilitate a more comprehensive understanding of the mechanisms of action of ICIs by enabling the assessment of receptor binding and biomarker accumulation (64, 65). Questions specific to a particular drug may be most effectively carried out by the drug developer, but both academic research groups and pharmaceutical companies could contribute to these studies. By understanding the uptake and distribution of drugs/molecules and their mechanisms of action, successful therapies may be identified earlier, with higher confidence (in “go”/“no-go” decisions), leading to lower development costs (64, 65).

In conclusion, PD-(L)1 molecular imaging offers the exciting opportunity to improve patient care by offering a non-invasive, dynamic technique to diagnose, select, and monitor patients based on PD-(L)1 expression, and to aid the development of immunotherapies.

AUTHOR CONTRIBUTIONS

All authors listed have made a substantial, direct, and intellectual contribution to the work, and approved it for publication.

ACKNOWLEDGMENTS

Medical writing support and editorial assistance were provided by Sarah Pinder, PhD, and Jay Rathi, MA, of Spark Medica Inc,

REFERENCES

1. Yan X, Zhang S, Deng Y, Wang P, Hou Q, Xu H. Prognostic Factors for Checkpoint Inhibitor Based Immunotherapy: An Update With New Evidences. *Front Pharmacol* (2018) 9:1050. doi: 10.3389/fphar.2018.01050
2. Du Y, Jin Y, Sun W, Fang J, Zheng J, Tian J. Advances in Molecular Imaging of Immune Checkpoint Targets in Malignancies: Current and Future Prospect. *Eur Radiol* (2019) 29(8):4294–302. doi: 10.1007/s00330-018-5814-3
3. Chen S, Crabill GA, Pritchard TS, McMiller TL, Wei P, Pardoll DM, et al. Mechanisms Regulating PD-L1 Expression on Tumor and Immune Cells. *J Immunother Cancer* (2019) 7(1):305. doi: 10.1186/s40425-019-0770-2
4. Schmidt EV. Developing Combination Strategies Using PD-1 Checkpoint Inhibitors to Treat Cancer. *Semin Immunopathol* (2019) 41(1):21–30. doi: 10.1007/s00281-018-0714-9
5. Anceschi Hunter K, Socinski MA, Villaruz LC. PD-L1 Testing in Guiding Patient Selection for PD-1/PD-L1 Inhibitor Therapy in Lung Cancer. *Mol Diagn Ther* (2018) 22(1):1–10. doi: 10.1007/s40291-017-0308-6
6. Keir ME, Butte MJ, Freeman GJ, Sharpe AH. PD-1 and Its Ligands in Tolerance and Immunity. *Annu Rev Immunol* (2008) 26:677–704. doi: 10.1146/annurev.immunol.26.021607.090331
7. Wang Q, Liu F, Liu L. Prognostic Significance of PD-L1 in Solid Tumor: An Updated Meta-Analysis. *Medicine* (2017) 96(18):e6369. doi: 10.1097/MD.00000000000006369
8. Taube JM, Klein A, Brahmer JR, Xu H, Pan X, Kim JH, et al. Association of PD-1, PD-1 Ligands, and Other Features of the Tumor Immune Microenvironment With Response to Anti-PD-1 Therapy. *Clin Cancer Res* (2014) 20(19):5064–74. doi: 10.1158/1078-0432.Ccr-13-3271
9. Mazzaschi G, Madeddu D, Falco A, Bocchialini G, Goldoni M, Sogni F, et al. Low PD-1 Expression in Cytotoxic CD8+ Tumor-Infiltrating Lymphocytes Confers an Immune-Privileged Tissue Microenvironment in NSCLC With a Prognostic and Predictive Value. *Clin Cancer Res* (2018) 24(2):407–19. doi: 10.1158/1078-0432.Ccr-17-2156
10. Büttner R, Gosney JR, Skov BG, Adam J, Motoi N, Bloom KJ, et al. Programmed Death-Ligand 1 Immunohistochemistry Testing: A Review of Analytical Assays and Clinical Implementation in Non-Small-Cell Lung Cancer. *J Clin Oncol* (2017) 35(34):3867–76. doi: 10.1200/JCO.2017.74.7642
11. Cole EL, Kim J, Donnelly DJ, Smith RA, Cohen D, Lafont V, et al. Radiosynthesis and Preclinical PET Evaluation of (89)Zr-Nivolumab (BMS-936558) in Healthy Non-Human Primates. *Bioorg Med Chem* (2017) 25(20):5407–14. doi: 10.1016/j.bmc.2017.07.066
12. Donnelly DJ, Smith RA, Morin P, Lipovsek D, Gokemeijer J, Cohen D, et al. Synthesis and Biologic Evaluation of a Novel (18)F-Labeled Adnectin as a PET Radioligand for Imaging PD-L1 Expression. *J Nucl Med* (2018) 59(3):529–35. doi: 10.2967/jnumed.117.199596
13. Lv G, Sun X, Qiu L, Sun Y, Li K, Liu Q, et al. PET Imaging of Tumor PD-L1 Expression With a Highly Specific Nonblocking Single-Domain Antibody. *J Nucl Med* (2020) 61(1):117–22. doi: 10.2967/jnumed.119.226712
14. Heskamp S, Hobo W, Molkenboer-Kuening JD, Olive D, Oyen WJ, Dolstra H, et al. Noninvasive Imaging of Tumor PD-L1 Expression Using Radiolabeled Anti-PD-L1 Antibodies. *Cancer Res* (2015) 75(14):2928–36. doi: 10.1158/0008-5472.Can-14-3477
15. Natarajan A, Mayer AT, Xu L, Reeves RE, Gano J, Gambhir SS. Novel Radiotracer for ImmunoPET Imaging of PD-1 Checkpoint Expression on Tumor Infiltrating Lymphocytes. *Bioconjug Chem* (2015) 26(10):2062–9. doi: 10.1021/acs.bioconjchem.5b00318
16. Josefsson A, Nedrow JR, Park S, Banerjee SR, Rittenbach A, Jammes F, et al. Imaging, Biodistribution, and Dosimetry of Radionuclide-Labeled PD-L1 Antibody in an Immunocompetent Mouse Model of Breast Cancer. *Cancer Res* (2016) 76(2):472–9. doi: 10.1158/0008-5472.Can-15-2141
17. Lesniak WG, Chatterjee S, Gabrielson M, Lisok A, Wharram B, Pomper MG, et al. PD-L1 Detection in Tumors Using [(64)Cu]Atezolizumab With PET. *Bioconjug Chem* (2016) 27(9):2103–10. doi: 10.1021/acs.bioconjchem.6b00348
18. Chatterjee S, Lesniak WG, Miller MS, Lisok A, Sikorska E, Wharram B, et al. Rapid PD-L1 Detection in Tumors With PET Using a Highly Specific Peptide. *Biochem Biophys Res Commun* (2017) 483(1):258–63. doi: 10.1016/j.bbrc.2016.12.156
19. Chatterjee S, Lesniak WG, Gabrielson M, Lisok A, Wharram B, Sysa-Shah P, et al. A Humanized Antibody for Imaging Immune Checkpoint Ligand PD-L1 Expression in Tumors. *Oncotarget* (2016) 7(9):10215–27. doi: 10.18632/oncotarget.7143
20. Vaz SC, Capacho AS, Oliveira FP, Gil N, Barros CT, Parreira A, et al. Radiopharmacology and Molecular Imaging of PD-L1 Expression in Cancer. *Clin Transl Imaging* (2018) 6:429–39. doi: 10.1007/s40336-018-0303-x
21. Broos K, Lecocq Q, Raes G, Devoogdt N, Keyaerts M, Breckpot K. Noninvasive Imaging of the PD-1:PD-L1 Immune Checkpoint: Embracing Nuclear Medicine for the Benefit of Personalized Immunotherapy. *Theranostics* (2018) 8(13):3559–70. doi: 10.7150/thno.24762
22. Brahmer J, Reckamp KL, Baas P, Crino L, Eberhardt WEE, Poddubskaya E, et al. Nivolumab Versus Docetaxel in Advanced Squamous-Cell Non-Small-Cell Lung Cancer. *N Engl J Med* (2015) 373(2):123–35. doi: 10.1056/NEJMoa1504627
23. Borghaei H, Paz-Ares L, Horn L, Spigel DR, Steins M, Ready NE, et al. Nivolumab Versus Docetaxel in Advanced Nonsquamous Non-Small-Cell Lung Cancer. *N Engl J Med* (2015) 373(17):1627–39. doi: 10.1056/NEJMoa1507643
24. Herbst RS, Baas P, Perez-Gracia JL, Felip E, Kim D-W, Han J-Y, et al. Use of Archival Versus Newly Collected Tumor Samples for Assessing PD-L1 Expression and Overall Survival: An Updated Analysis of KEYNOTE-010 Trial. *Ann Oncol* (2019) 30(2):281–9. doi: 10.1093/annonc/mdy545
25. Ilie M, Long-Mira E, Bence C, Butori C, Lassalle S, Bouhlef L, et al. Comparative Study of the PD-L1 Status Between Surgically Resected Specimens and Matched Biopsies of NSCLC Patients Reveal Major Discordances: A Potential Issue for Anti-PD-L1 Therapeutic Strategies. *Ann Oncol* (2016) 27(1):147–53. doi: 10.1093/annonc/mdv489
26. Munari E, Zamboni G, Marconi M, Sommaggio M, Brunelli M, Martignoni G, et al. PD-L1 Expression Heterogeneity in Non-Small Cell Lung Cancer: Evaluation of Small Biopsies Reliability. *Oncotarget* (2017) 8(52):90123–31. doi: 10.18632/oncotarget.21485
27. Waaiaer SJH, Kok IC, Eisses B, Schroder CP, Jalving M, Brouwers AH, et al. Molecular Imaging in Cancer Drug Development. *J Nucl Med* (2018) 59(5):726–32. doi: 10.2967/jnumed.116.188045
28. Verhoeff SR, van den Heuvel MM, van Herpen CML, Piet B, Aarntzen E, Heskamp S. Programmed Cell Death-1/Ligand-1 PET Imaging: A Novel Tool to Optimize Immunotherapy? *PET Clin* (2020) 15(1):35–43. doi: 10.1016/j.cpet.2019.08.008
29. Jørgensen JT, Nielsen KB. Companion and Complementary Diagnostics for First-Line Immune Checkpoint Inhibitor Treatment in Non-Small Cell Lung

funded by Bristol Myers Squibb, according to Good Publication Practice guidelines.

SUPPLEMENTARY MATERIAL

The Supplementary Material for this article can be found online at: <https://www.frontiersin.org/articles/10.3389/fonc.2021.698425/full#supplementary-material>

- Cancer. *Transl Lung Cancer Res* (2018) 7(suppl 2):S95–S9. doi: 10.21037/tlcr.2018.02.08
30. Udall M, Rizzo M, Kenny J, Doherty J, Dahm S, Robbins P, et al. PD-L1 Diagnostic Tests: A Systematic Literature Review of Scoring Algorithms and Test-Validation Metrics. *Diagn Pathol* (2018) 13(1):12. doi: 10.1186/s13000-018-0689-9
 31. Scheel AH, Dietel M, Heukamp LC, Johrens K, Kirchner T, Reu S, et al. Harmonized PD-L1 Immunohistochemistry for Pulmonary Squamous-Cell and Adenocarcinomas. *Mod Pathol* (2016) 29(10):1165–72. doi: 10.1038/modpathol.2016.117
 32. Zajac M, Scott M, Ratcliffe M, Scorer P, Barker C, Al-Masri H, et al. Concordance Among Four Commercially Available, Validated Programmed Cell Death Ligand-1 Assays in Urothelial Carcinoma. *Diagn Pathol* (2019) 14(1):99. doi: 10.1186/s13000-019-0873-6
 33. McLaughlin J, Han G, Schalper KA, Carvajal-Hausdorf D, Pelekanou V, Rehman J, et al. Quantitative Assessment of the Heterogeneity of PD-L1 Expression in Non-Small-Cell Lung Cancer. *JAMA Oncol* (2016) 2(1):46–54. doi: 10.1001/jamaoncol.2015.3638
 34. Bera K, Schalper KA, Rimm DL, Velcheti V, Madabhushi A. Artificial Intelligence in Digital Pathology - New Tools for Diagnosis and Precision Oncology. *Nat Rev Clin Oncol* (2019) 16(11):703–15. doi: 10.1038/s41571-019-0252-y
 35. Miele E, Spinelli GP, Tomao F, Zullo A, De Marinis F, Pasciuti G, et al. Positron Emission Tomography (PET) Radiotracers in Oncology—Utility of 18F-Fluoro-Deoxy-Glucose (FDG)-PET in the Management of Patients With Non-Small-Cell Lung Cancer (NSCLC). *J Exp Clin Cancer Res* (2008) 27:52. doi: 10.1186/1756-9966-27-52
 36. Anand SS, Singh H, Dash AK. Clinical Applications of PET and PET-CT. *Med J Armed Forces India* (2009) 65(4):353–8. doi: 10.1016/s0377-1237(09)80099-3
 37. Lazzari R, Cecconi A, Jereczek-Fossa BA, Travaini LL, Dell'Acqua V, Cattani F, et al. The Role of [(18)F]FDG-PET/CT in Staging and Treatment Planning for Volumetric Modulated Rapidarc Radiotherapy in Cervical Cancer: Experience of the European Institute of Oncology, Milan, Italy. *Ecancermedicalscience* (2014) 8:405. doi: 10.3332/ecancer.2014.409
 38. Cuaron J, Dunphy M, Rimmer A. Role of FDG-PET Scans in Staging, Response Assessment, and Follow-Up Care for Non-Small Cell Lung Cancer. *Front Oncol* (2012) 2:208. doi: 10.3389/fonc.2012.00208
 39. Seban RD, Moya-Plana A, Antonios L, Yeh R, Marabelle A, Deutsch E, et al. Prognostic 18f-FDG PET Biomarkers in Metastatic Mucosal and Cutaneous Melanoma Treated With Immune Checkpoint Inhibitors Targeting PD-1 and CTLA-4. *Eur J Nucl Med Mol Imaging* (2020) 47(10):2301–12. doi: 10.1007/s00259-020-04757-3
 40. Ito K, Schoder H, Teng R, Humm JL, Ni A, Wolchok JD, et al. Prognostic Value of Baseline Metabolic Tumor Volume Measured on (18)F-Fluorodeoxyglucose Positron Emission Tomography/Computed Tomography in Melanoma Patients Treated With Ipilimumab Therapy. *Eur J Nucl Med Mol Imaging* (2019) 46(4):930–9. doi: 10.1007/s00259-018-4211-0
 41. Kelloff GJ, Hoffman JM, Johnson B, Scher HI, Siegel BA, Cheng EY, et al. Progress and Promise of FDG-PET Imaging for Cancer Patient Management and Oncologic Drug Development. *Clin Cancer Res* (2005) 11(8):2785–808. doi: 10.1158/1078-0432.Ccr-04-2626
 42. Unterrainer M, Ruzicka M, Fabritius MP, Mittlmeier LM, Winkelmann M, Rubenthaler J, et al. PET/CT Imaging for Tumour Response Assessment to Immunotherapy: Current Status and Future Directions. *Eur Radiol Exp* (2020) 4(1):63. doi: 10.1186/s41747-020-00190-1
 43. Evangelista L, Cuppari L, Menis J, Bonanno L, Reccia P, Frega S, et al. 18f-FDG PET/CT in Non-Small-Cell Lung Cancer Patients: A Potential Predictive Biomarker of Response to Immunotherapy. *Nucl Med Commun* (2019) 40(8):802–7. doi: 10.1097/mnm.0000000000001025
 44. Umeda Y, Morikawa M, Anzai M, Ameshima S, Kadowaki M, Waseda Y, et al. Predictive Value of Integrated (18)F-FDG PET/MRI in the Early Response to Nivolumab in Patients With Previously Treated Non-Small Cell Lung Cancer. *J Immunother Cancer* (2020) 8(1):e000349. doi: 10.1136/jitc-2019-000349
 45. Hashimoto K, Kaira K, Yamaguchi O, Mouri A, Shiono A, Miura Y, et al. Potential of FDG-PET as Prognostic Significance After Anti-PD-1 Antibody Against Patients With Previously Treated Non-Small Cell Lung Cancer. *J Clin Med* (2020) 9(3):725. doi: 10.3390/jcm9030725
 46. Chardin D, Paquet M, Schiappa R, Darcourt J, Bailleux C, Poudenx M, et al. Baseline Metabolic Tumor Volume as a Strong Predictive and Prognostic Biomarker in Patients With Non-Small Cell Lung Cancer Treated With PD1 Inhibitors: A Prospective Study. *J Immunother Cancer* (2020) 8(2):e000645. doi: 10.1136/jitc-2020-000645
 47. Seban RD, Assié JB, Giroux-Leprieur E, Massiani MA, Soussan M, Bonardel G, et al. Association of the Metabolic Score Using Baseline FDG-PET/CT and dNLR With Immunotherapy Outcomes in Advanced NSCLC Patients Treated With First-Line Pembrolizumab. *Cancers (Basel)* (2020) 12(8):2234. doi: 10.3390/cancers12082234
 48. Yamaguchi O, Kaira K, Hashimoto K, Mouri A, Shiono A, Miura Y, et al. Tumor Metabolic Volume by (18)F-FDG-PET as a Prognostic Predictor of First-Line Pembrolizumab for NSCLC Patients With PD-L1 ≥ 50 . *Sci Rep* (2020) 10(1):14990. doi: 10.1038/s41598-020-71735-y
 49. Zhao L, Liu J, Shi J, Wang H. Relationship Between SP142 PD-L1 Expression and (18)F-FDG Uptake in Non-Small-Cell Lung Cancer. *Contrast Media Mol Imaging* (2020) 2020:2010924. doi: 10.1155/2020/2010924
 50. Wang L, Ruan M, Lei B, Yan H, Sun X, Chang C, et al. The Potential of (18) F-FDG PET/CT in Predicting PDL1 Expression Status in Pulmonary Lesions of Untreated Stage IIIB-IV Non-Small-Cell Lung Cancer. *Lung Cancer (Amsterdam Netherlands)* (2020) 150:44–52. doi: 10.1016/j.lungcan.2020.10.004
 51. Chiou VL, Burotto M. Pseudoprogression and Immune-Related Response in Solid Tumors. *J Clin Oncol* (2015) 33(31):3541–3. doi: 10.1200/JCO.2015.61.6870
 52. Basler L, Gabrys HS, Hogan SA, Pavic M, Bogowicz M, Vuong D, et al. Radiomics, Tumor Volume, and Blood Biomarkers for Early Prediction of Pseudoprogression in Patients With Metastatic Melanoma Treated With Immune Checkpoint Inhibition. *Clin Cancer Res* (2020) 26(16):4414–25. doi: 10.1158/1078-0432.CCR-20-0020
 53. Im HJ, Pak K, Cheon GJ, Kang KW, Kim SJ, Kim IJ, et al. Prognostic Value of Volumetric Parameters of (18)F-FDG PET in Non-Small-Cell Lung Cancer: A Meta-Analysis. *Eur J Nucl Med Mol Imaging* (2015) 42(2):241–51. doi: 10.1007/s00259-014-2903-7
 54. Mokrane FZ, Chen A, Schwartz LH, Morschhauser F, Stamatoullas A, Schiano de Colella JM, et al. Performance of CT Compared With (18)F-FDG PET in Predicting the Efficacy of Nivolumab in Relapsed or Refractory Hodgkin Lymphoma. *Radiology* (2020) 295:651–61. doi: 10.1148/radiol.2020192056
 55. Chen A, Mokrane FZ, Schwartz LH, Morschhauser F, Stamatoullas A, Schiano de Colella JM, et al. Early (18)F-FDG PET/CT Response Predicts Survival in Relapsed or Refractory Hodgkin Lymphoma Treated With Nivolumab. *J Nucl Med* (2020) 61(5):649–54. doi: 10.2967/jnumed.119.232827
 56. Iravani A, Osman MM, Weppeler AM, Wallace R, Galligan A, Lasocki A, et al. FDG PET/CT for Tumoral and Systemic Immune Response Monitoring of Advanced Melanoma During First-Line Combination Ipilimumab and Nivolumab Treatment. *Eur J Nucl Med Mol Imaging* (2020) 47(12):2776–86. doi: 10.1007/s00259-020-04815-w
 57. van de Donk PP, Kist de Ruijter L, Lub-de Hooge MN, Brouwers AH, van der Wekken AJ, Oosting SF, et al. Molecular Imaging Biomarkers for Immune Checkpoint Inhibitor Therapy. *Theranostics* (2020) 10(4):1708–18. doi: 10.7150/thno.38339
 58. Donin NM, Reiter RE. Why Targeting PSMA Is a Game Changer in the Management of Prostate Cancer. *J Nucl Med* (2018) 59(2):177–82. doi: 10.2967/jnumed.117.191874
 59. Langbein T, Weber WA, Eiber M. Future of Theranostics: An Outlook on Precision Oncology in Nuclear Medicine. *J Nucl Med* (2019) 60(suppl 2):13s–9s. doi: 10.2967/jnumed.118.220566
 60. Dijkers EC, Kosterink JG, Rademaker AP, Perk LR, van Dongen GA, Bart J, et al. Development and Characterization of Clinical-Grade ^{89}Zr -Trastuzumab for HER2/neu immunoPET Imaging. *J Nucl Med* (2009) 50(6):974–81. doi: 10.2967/jnumed.108.060392
 61. McKnight BN, Viola-Villegas NT. ^{89}Zr -ImmunoPET Companion Diagnostics and Their Impact in Clinical Drug Development. *J Labelled Comp Radiopharm* (2018) 61:727–38. doi: 10.1002/jlcr.3605

62. Dijkers EC, Oude Munnink TH, Kosterink JG, Brouwers AH, Jager PL, de Jong JR, et al. Biodistribution of ⁸⁹Zr-Trastuzumab and PET Imaging of HER2-Positive Lesions in Patients With Metastatic Breast Cancer. *Clin Pharmacol Ther* (2010) 87(5):586–92. doi: 10.1038/clpt.2010.12
63. Metro G, Signorelli D. Immune Checkpoints Inhibitors Rechallenge in Non-Small-Cell Lung Cancer: Different Scenarios With Different Solutions? *Lung Cancer Manag* (2020) 8(4):LMT18. doi: 10.2217/lmt-2019-0012
64. Burt T, Yoshida K, Lappin G, Vuong L, John C, de Wildt SN, et al. Microdosing and Other Phase 0 Clinical Trials: Facilitating Translation in Drug Development. *Clin Transl Sci* (2016) 9(2):74–88. doi: 10.1111/cts.12390
65. Burke B, Archibald S. *Applications of Molecular Imaging in Drug Development* (2018). Available at: <https://www.drugtargetreview.com/article/33698/applications-of-molecular-imaging-in-drug-development-2/> (Accessed April 19, 2021).
66. Tamura K, Kurihara H, Yonemori K, Tsuda H, Suzuki J, Kono Y, et al. ⁶⁴Cu-DOTA-Trastuzumab PET Imaging in Patients With HER2-Positive Breast Cancer. *J Nucl Med* (2013) 54(11):1869–75. doi: 10.2967/jnumed.112.118612
67. International Atomic Energy Agency. *A Guide to Clinical PET in Oncology: Improving Clinical Management of Cancer Patients* (2008). Available at: https://www-pub.iaea.org/MTCD/Publications/PDF/te_1605_web.pdf (Accessed April 19, 2021).
68. de Vries EGE, Kist de Ruijter L, Lub-de Hooge MN, Dierckx RA, Elias SG, Oosting SF. Integrating Molecular Nuclear Imaging in Clinical Research to Improve Anticancer Therapy. *Nat Rev Clin Oncol* (2019) 16(4):241–55. doi: 10.1038/s41571-018-0123-y
69. Kelly RJ, Turner R, Chen YW, Rigas JR, Fernandes AW, Karve S. Complications and Economic Burden Associated With Obtaining Tissue for Diagnosis and Molecular Analysis in Patients With Non-Small-Cell Lung Cancer in the United States. *J Oncol Pract* (2019) 15(8):e717–27. doi: 10.1200/jop.18.00762
70. Raab SS. The Cost-Effectiveness of Immunohistochemistry. *Arch Pathol Lab Med* (2000) 124(8):1185–91. doi: 10.5858/2000-124-1185-TCEOI
71. Xing Y, Chand G, Liu C, Cook GJR, O'Doherty J, Zhao L, et al. Early Phase I Study of a (^{99m}Tc)-Labeled Anti-Programmed Death Ligand-1 (PD-L1) Single-Domain Antibody in SPECT/CT Assessment of PD-L1 Expression in Non-Small Cell Lung Cancer. *J Nucl Med* (2019) 60(9):1213–20. doi: 10.2967/jnumed.118.224170
72. Niemeijer AN, Leung D, Huisman MC, Bahce I, Hoekstra OS, van Dongen G, et al. Whole Body PD-1 and PD-L1 Positron Emission Tomography in Patients With Non-Small-Cell Lung Cancer. *Nat Commun* (2018) 9(1):4664. doi: 10.1038/s41467-018-07131-y
73. Bensch F, van der Veen EL, Lub-de Hooge MN, Jorritsma-Smit A, Boellaard R, Kok IC, et al. (⁸⁹Zr)-Atezolizumab Imaging as a Non-Invasive Approach to Assess Clinical Response to PD-L1 Blockade in Cancer. *Nat Med* (2018) 24(12):1852–8. doi: 10.1038/s41591-018-0255-8
74. Kim H, Chung JH. PD-L1 Testing in Non-Small Cell Lung Cancer: Past, Present, and Future. *J Pathol Transl Med* (2019) 53(4):199–206. doi: 10.4132/jptm.2019.04.24
75. Kulangara K, Zhang N, Corigliano E, Guerrero L, Waldroup S, Jaiswal D, et al. Clinical Utility of the Combined Positive Score for Programmed Death Ligand-1 Expression and the Approval of Pembrolizumab for Treatment of Gastric Cancer. *Arch Pathol Lab Med* (2019) 143(3):330–7. doi: 10.5858/arpa.2018-0043-OA
76. Schillaci O, Scimeca M, Toschi N, Bonfiglio R, Urbano N, Bonanno E. Combining Diagnostic Imaging and Pathology for Improving Diagnosis and Prognosis of Cancer. *Contrast Media Mol Imaging* (2019) 2019:9429761. doi: 10.1155/2019/9429761
77. Maute RL, Gordon SR, Mayer AT, McCracken MN, Natarajan A, Ring NG, et al. Engineering High-Affinity PD-1 Variants for Optimized Immunotherapy and Immuno-PET Imaging. *Proc Natl Acad Sci USA* (2015) 112(47):E6506–E14. doi: 10.1073/pnas.1519623112
78. Mayer AT, Natarajan A, Gordon SR, Maute RL, McCracken MN, Ring AM, et al. Practical Immuno-PET Radiotracer Design Considerations for Human Immune Checkpoint Imaging. *J Nucl Med* (2017) 58(4):538–46. doi: 10.2967/jnumed.116.177659
79. Kuchar M, Mamat C. Methods to Increase the Metabolic Stability of (¹⁸F)-Radiotracers. *Molecules* (2015) 20(9):16186–220. doi: 10.3390/molecules200916186
80. Kraeber-Bodere F, Rousseau C, Bodet-Milin C, Mathieu C, Guerard F, Frampas E, et al. Tumor Immunotargeting Using Innovative Radionuclides. *Int J Mol Sci* (2015) 16(2):3932–54. doi: 10.3390/ijms16023932
81. Vazquez-Lombardi R, Phan TG, Zimmermann C, Lowe D, Jermutus L, Christ D. Challenges and Opportunities for Non-Antibody Scaffold Drugs. *Drug Discovery Today* (2015) 20(10):1271–83. doi: 10.1016/j.drudis.2015.09.004
82. Li Z, Krippendorff BF, Sharma S, Walz AC, Lavé T, Shah DK. Influence of Molecular Size on Tissue Distribution of Antibody Fragments. *MAbs* (2016) 8(1):113–9. doi: 10.1080/19420862.2015.1111497
83. Grassi I, Nanni C, Allegri V, Morigi JJ, Montini GC, Castellucci P, et al. The Clinical Use of PET With (¹¹C)-Acetate. *Am J Nucl Med Mol Imaging* (2012) 2(1):33–47.
84. Solomon AK. Half-Life of C11. *Phys Rev* (1941) 60:279. doi: 10.1103/PhysRev.60.279
85. Boellaard R, O'Doherty MJ, Weber WA, Mottaghy FM, Lonsdale MN, Stroobants SG, et al. FDG PET and PET/CT: EANM Procedure Guidelines for Tumour PET Imaging: Version 1.0. *Eur J Nucl Med Mol Imaging* (2010) 37(1):181–200. doi: 10.1007/s00259-009-1297-4
86. Stutvoet TS, van der Veen EL, Kol A, Antunes IF, de Vries EFJ, Hospers GAP, et al. Molecular Imaging of PD-L1 Expression and Dynamics With the Adnectin-Based PET Tracer (¹⁸F)-BMS-986192. *J Nucl Med* (2020) 61(12):1839–44. doi: 10.2967/jnumed.119.241364
87. Yoon J-K, Park B-N, Ryu E-K, An Y-S, Lee S-J. Current Perspectives on (⁸⁹Zr)-PET Imaging. *Int J Mol Sci* (2020) 21(12):4309. doi: 10.3390/ijms21124309
88. Badawi RD, Shi H, Hu P, Chen S, Xu T, Price PM, et al. First Human Imaging Studies With the EXPLORER Total-Body PET Scanner. *J Nucl Med* (2019) 60(3):299–303. doi: 10.2967/jnumed.119.226498
89. Berg E, Gill H, Marik J, Ogasawara A, Williams S, van Dongen G, et al. Total-Body PET and Highly Stable Chelators Together Enable Meaningful (⁸⁹Zr)-Antibody PET Studies Up to 30 Days After Injection. *J Nucl Med* (2020) 61(3):453–60. doi: 10.2967/jnumed.119.230961
90. Cherry SR, Jones T, Karp JS, Qi J, Moses WW, Badawi RD. Total-Body PET: Maximizing Sensitivity to Create New Opportunities for Clinical Research and Patient Care. *J Nucl Med* (2018) 59(1):3–12. doi: 10.2967/jnumed.116.184028
91. Jauw YW, Menke-Van Der Houven Van Oordt CW, Hoekstra OS, Hendrikse NH, Vugts DJ, Zijlstra JM, et al. Immuno-Positron Emission Tomography With Zirconium-89-Labeled Monoclonal Antibodies in Oncology: What can We Learn From Initial Clinical Trials? *Front Pharmacol* (2016) 7:131. doi: 10.3389/fphar.2016.00131
92. McCluskey SP, Plisson C, Rabiner EA, Howes O. Advances in CNS PET: The State-of-the-Art for New Imaging Targets for Pathophysiology and Drug Development. *Eur J Nucl Med Mol Imaging* (2020) 47(2):451–89. doi: 10.1007/s00259-019-04488-0
93. Rahmim A, Zaidi H. PET Versus SPECT: Strengths, Limitations and Challenges. *Nucl Med Commun* (2008) 29(3):193–207. doi: 10.1097/MNM.0b013e3282f3a515
94. Muzi M, O'Sullivan F, Mankoff DA, Doot RK, Pierce LA, Kurland BF, et al. Quantitative Assessment of Dynamic PET Imaging Data in Cancer Imaging. *Magn Reson Imaging* (2012) 30(9):1203–15. doi: 10.1016/j.mri.2012.05.008
95. Jauw YWS, O'Donoghue JA, Zijlstra JM, Hoekstra OS, Menke-van der Houven van Oordt CW, Morschhauser F, et al. (⁸⁹Zr)-Immuno-PET: Toward a Noninvasive Clinical Tool to Measure Target Engagement of Therapeutic Antibodies *In Vivo*. *J Nucl Med* (2019) 60(12):1825–32. doi: 10.2967/jnumed.118.224568
96. Rahmim A, Lodge MA, Karakatsanis NA, Panin VY, Zhou Y, McMillan A, et al. Dynamic Whole-Body PET Imaging: Principles, Potentials and Applications. *Eur J Nucl Med Mol Imaging* (2019) 46(2):501–18. doi: 10.1007/s00259-018-4153-6
97. Hettich M, Braun F, Bartholoma MD, Schirmbeck R, Niedermann G. High-Resolution PET Imaging With Therapeutic Antibody-Based PD-1/PD-L1 Checkpoint Tracers. *Theranostics* (2016) 6(10):1629–40. doi: 10.7150/thno.15253
98. England CG, Ehlerding EB, Hernandez R, Rekoske BT, Graves SA, Sun H, et al. Preclinical Pharmacokinetics and Biodistribution Studies of ⁸⁹Zr-Labeled Pembrolizumab. *J Nucl Med* (2017) 58(1):162–8. doi: 10.2967/jnumed.116.177857

99. Verhoeff S, Donk PPVD, Aarntzen EHJG, Miedema IHC, Oosting S, Voortman J, et al. ^{89}Zr -Durvalumab PD-L1 PET in Recurrent or Metastatic (R/M) Squamous Cell Carcinoma of the Head and Neck. *J Clin Oncol* (2020) 38(suppl 15):3573. doi: 10.1200/JCO.2020.38.15_suppl.3573
100. Huisman M, Niemeijer AL, Windhorst B, Schuit R, Leung D, Hayes W, et al. Quantification of PD-L1 Expression With [(18)F]BMS-986192 PET/CT in Patients With Advanced Stage Non-Small-Cell Lung Cancer. *J Nucl Med* (2020) 61(10):1455–60. doi: 10.2967/jnumed.119.240895
101. Nedrow JR, Josefsson A, Park S, Ranka S, Roy S, Sgouros G. Imaging of Programmed Cell Death Ligand 1: Impact of Protein Concentration on Distribution of Anti-PD-L1 SPECT Agents in an Immunocompetent Murine Model of Melanoma. *J Nucl Med* (2017) 58(10):1560–6. doi: 10.2967/jnumed.117.193268
102. Mirus M, Tokalov SV, Abramyuk A, Heindol J, Prochnow V, Zophel K, et al. Noninvasive Assessment and Quantification of Tumor Vascularization Using [18F]FDG-PET/CT and CE-CT in a Tumor Model With Modifiable Angiogenesis—an Animal Experimental Prospective Cohort Study. *EJNMMI Res* (2019) 9(1):55. doi: 10.1186/s13550-019-0502-0
103. Hughes DJ, Chand G, Goh V, Cook GJR. Inter- and Intraobserver Agreement of the Quantitative Assessment of [(99m)Tc]-Labelled Anti-Programmed Death-Ligand 1 (PD-L1) SPECT/CT in Non-Small Cell Lung Cancer. *EJNMMI Res* (2020) 10(1):145. doi: 10.1186/s13550-020-00734-x
104. Lohrmann C, O'Reilly EM, O'Donoghue JA, Pandit-Taskar N, Carrasquillo JA, Lyashchenko SK, et al. Retooling a Blood-Based Biomarker: Phase I Assessment of the High-Affinity CA19-9 Antibody HuMab-5B1 for Immuno-PET Imaging of Pancreatic Cancer. *Clin Cancer Res* (2019) 25(23):7014–23. doi: 10.1158/1078-0432.CCR-18-3667
105. Robu S, Richter A, Gosmann D, Seidl C, Leung D, Hayes W, et al. Synthesis and Preclinical Evaluation of (68)Ga-Labeled Adnectin, (68)Ga-BMS-986192 as a PET Agent for Imaging PD-L1 Expression. *J Nucl Med* (2021). doi: 10.2967/jnumed.120.258384
106. US Food and Drug Administration. Guidance for Industry, Investigators, and Reviewers: Exploratory IND Studies. Rockville, MD, USA (2006).
107. OECD/NEA. *The Supply of Medical Isotopes: An Economic Diagnosis and Possible Solutions* (2019). Available at: <http://www.oecd-nea.org/ndd/pubs/2019/medical-radioisotope-supply.pdf> (Accessed April 19, 2021).
108. Green CH. Technetium-99m Production Issues in the United Kingdom. *J Med Phys* (2012) 37(2):66–71. doi: 10.4103/0971-6203.94740
109. Woodcock J, Woosley R. The FDA Critical Path Initiative and Its Influence on New Drug Development. *Annu Rev Med* (2008) 59:1–12. doi: 10.1146/annurev.med.59.090506.155819
110. Kato T, Shinoda J, Nakayama N, Miwa K, Okumura A, Yano H, et al. Metabolic Assessment of Gliomas Using 11C-Methionine, [18F] Fluorodeoxyglucose, and 11C-Choline Positron-Emission Tomography. *AJNR Am J Neuroradiol* (2008) 29(6):1176–82. doi: 10.3174/ajnr.A1008
111. Li Y, Zhang W, Wu H, Liu G. Advanced Tracers in PET Imaging of Cardiovascular Disease. *BioMed Res Int* (2014) 2014:504532. doi: 10.1155/2014/504532
112. Hu ZI, McArthur HL, Ho AY. The Abscopal Effect of Radiation Therapy: What Is It and How can We Use It in Breast Cancer? *Curr Breast Cancer Rep* (2017) 9(1):45–51. doi: 10.1007/s12609-017-0234-y
113. Marciscano AE, Thorek DLJ. Role of Noninvasive Molecular Imaging in Determining Response. *Adv Radiat Oncol* (2018) 3(4):534–47. doi: 10.1016/j.adro.2018.07.006
114. Abu Hejleh T, Furqan M, Ballas Z, Clamon G. The Clinical Significance of Soluble PD-1 and PD-L1 in Lung Cancer. *Crit Rev Oncol Hematol* (2019) 143:148–52. doi: 10.1016/j.critrevonc.2019.08.009
115. Baxi V, Beck A, Pandya D, Lee G, Hedvat C, Khosla A, et al. Artificial Intelligence-Powered Retrospective Analysis of PD-L1 Expression in Nivolumab Trials of Advanced Non-Small Cell Lung Cancer. *J Immunother Cancer* (2019) 7(suppl 1):O65. doi: 10.1186/s40425-019-0764-0
116. Beck A, Glass B, Elliott H, Kerner JK, Khosla A, Lahiri A, et al. An Empirical Framework for Validating Artificial Intelligence-Derived PD-L1 Positivity Predictions Applied to Urothelial Carcinoma. *J Immunother Cancer* (2019) 7(suppl 1):P730. doi: 10.1186/s40425-019-0764-0

Conflict of Interest: DL, SB, and RS are employees of, and hold stock and shares in, Bristol Myers Squibb. WH was employed by Bristol Myers Squibb at the time the manuscript was drafted, and holds stock and shares in Bristol Myers Squibb. WW is on advisory boards for, and receives compensation from, Bayer, Blue Earth Diagnostics, Endocyte, ITM, and Pentixapharm, and has received research support from Bristol Myers Squibb, ImaginAb, Ipsen, and Piramal.

Publisher's Note: All claims expressed in this article are solely those of the authors and do not necessarily represent those of their affiliated organizations, or those of the publisher, the editors and the reviewers. Any product that may be evaluated in this article, or claim that may be made by its manufacturer, is not guaranteed or endorsed by the publisher.

Copyright © 2021 Leung, Bonacorsi, Smith, Weber and Hayes. This is an open-access article distributed under the terms of the Creative Commons Attribution License (CC BY). The use, distribution or reproduction in other forums is permitted, provided the original author(s) and the copyright owner(s) are credited and that the original publication in this journal is cited, in accordance with accepted academic practice. No use, distribution or reproduction is permitted which does not comply with these terms.